Structural Studies of Λ- and Δ-[Ru(phen)$_2$dppz]$^{2+}$ Bound to d(GTCGAC)$_2$: Characterization of Enantioselective Intercalation

Cynthia M. Dupureur[†] and Jacqueline K. Barton*

Beckman Institute, California Institute of Technology, Pasadena, California 91125

Received June 20, 1996[⊗]

^{1}H and ^{31}P NMR spectroscopies have been applied in the structural characterization of the enantioselective interactions between Λ- and Δ-[Ru(phen)$_2$dppz]$^{2+}$ (dppz = dipyridophenazine) and the hexamer oligonucleotide d(GTCGAC)$_2$. Issues of intercalation, exchange rate, sequence specificity, enantioselectivity, and the distribution of binding geometries have been explored. Several forms of evidence support intercalation by both isomers: (i) upfield changes in ^{1}H chemical shift for protons of the dppz ligand; (ii) characteristic downfield changes in ^{31}P chemical shifts for the duplex bound by the metal complex; (iii) increases in duplex melting temperature in the presence of both isomers. Slow exchange is achieved near 0 °C, thus permitting the observation of individual binding events. While both isomers intercalate into the helix, enantioselective differences in intercalation are evident. Differences in intercalative geometries are clearly manifested through chiral shifts in racemic mixtures and distinct resonance patterns for the 4′,7′-dppz ligand protons of Λ- and Δ-[Ru(phen-d_8)$_2$dppz]$^{2+}$. Intermolecular NOEs place the Δ-isomer in the major groove. For the Λ-isomer, substantially broader lines are evident, reflecting clear differences in the diastereomeric interactions. The Λ-isomer bound to DNA exhibits behavior consistent with a faster exchange rate compared to the Δ-isomer and/or a low level of sequence selectivity under NMR conditions. Similar characteristics of intercalation for both isomers are evident upon fluorine substitution onto the distal end of the dppz ligand; based upon chemical shift changes, it appears that fluorine substitution leads to a deeper stacking interaction. The movement of dppz ligand proton resonances upon binding DNA also indicates that [Ru(phen)$_2$dppz]$^{2+}$ isomers bind to the DNA helix with a population of intercalative geometries, some of which provide asymmetric protection of the dppz ligand from aqueous solvent. These results therefore support and extend earlier structural models based upon luminescence studies.

There is a wealth of activity and interest in understanding and developing the DNA binding properties of ruthenium(II) polypyridyls.[1−6] The luminescent characteristics of ruthenium complexes and their perturbations on binding to DNA have led to their general application as spectroscopic probes for nucleic acids. Among these intercalators, [Ru(phen)$_2$dppz]$^{2+}$ has shown the most promise in diagnostic applications which target nucleic acids.[1,6] Quenched in aqueous solution, [Ru(phen)$_2$dppz]$^{2+}$ luminesces brightly when intercalated into DNA. This luminescent characteristic, coupled with high binding affinity for DNA ($K_a \approx 10^6$ M^{-1}) permits the application of [Ru(phen)$_2$dppz]$^{2+}$ as a nonradioactive probe of double-stranded DNA at analytical concentrations. Dppz complexes of Os(II)[7] and Re(I)[8] have also been prepared and show DNA-dependent luminescence with distinct spectroscopic characteristics. Furthermore, the unique electronics of the dppz complexes make them suitable photoinduced donors to intercalated [Rh(phi)]$^{3+}$ (phi = phenanthrenequinone diimine) complexes in DNA-mediated electron transfer reactions.[9] Importantly, the luminescence of the dppz complexes appear to be quite sensitive to the geometry of stacking between the dppz ligand and DNA base pairs. Hence it becomes essential to develop a structural understanding of the intercalation of dppz complexes in DNA.

Despite wide interest in these complexes, there is currently little information concerning DNA site-specificity and intercalative geometries of dppz complexes. To date, most of what is known about [Ru(phen)$_2$dppz]$^{2+}$−DNA interactions originates from results obtained using luminescence spectroscopy.[2,6−8,10,11] The extent to which the luminescence of DNA-bound ruthenium is quenched in buffer, as manifested in its luminescence decay lifetimes, correlates with the degree of protection of the phenazine nitrogens from aqueous solvent afforded by various

* Author to whom correspondence should be addressed.
[†]Present address: Department of Biochemistry and Biophysics, Texas A&M University, College Station, TX 77843.
[⊗] Abstract published in *Advance ACS Abstracts,* December 15, 1996.

(1) (a) Murphy, C. J.; Barton, J. K. *Meth. Enzymol.* **1993**, *226*, 570. (b) Turro, N. J.; Tomalia, D. A.; Barton, J. K. *Acc. Chem. Res.* **1991**, *24*, 332.
(2) Friedman, A. E.; Chambron, J.-C.; Sauvage, J.-P.; Turro, N. J.; Barton, J. K. *J. Am. Chem. Soc.* **1990,** *112*, 4960.
(3) (a) Bannwarth, W.; Schmidt, D.; Stallard, R. L.; Hornung, C.; Knorr, R.; Muller, F. *Helvet. Chim. Acta* **1988**, *71*, 2085. (b) Tessler, J.; Cruickshank, K. A.; Morrison, L. E.; Netzel. T. L.; Chan, C. *J. Am. Chem. Soc.* **1989,** *111*, 7226.
(4) (a) Grover, N.; Gupta, N.; Thorp, H. H. *J. Am. Chem. Soc.* **1992,** *114*, 3390. (b) Smith, S. R.; Neyhart, G. A.; Kalsbeck, W. A.; Thorp, H. H. *New J. Chem.* **1992,** *18*, 397.
(5) Lecomte, J.-P.; Kirsch- De Mesmaeker, A.; Feeney, M. M.; Kelly, J. M. *Inorg. Chem.* **1995**, *34*, 6481.
(6) (a) Jenkins, Y.; Friedman, A. E.; Turro, N. J.; Barton, J. K. *Biochemistry* **1992**, *31*, 10809. (b) Hartshorn, R. M.; Barton, J. K. *J. Am. Chem. Soc.* **1992**, *114*, 5919. (c) Hiort, C.; Lincoln, P.; Norden, B. *J. Am. Chem. Soc.* **1993**, *115*, 3448. (d) Jenkins, Y.; Barton, J. K. *J. Am. Chem. Soc.* **1992**, *114*, 8736.
(7) (a) Holmlin, R. E.; Barton, J. K. *Inorg. Chem.* **1995**, *34*, 7. (b) Holmlin, R. E.; Stemp, E. D. A.; Barton, J. K. *J. Am. Chem. Soc.* **1996**, *118*, 5236.
(8) Stoeffler, H. D.; Thornton, N. B.; Temkin, S. L.; Schanze, K. S. *J. Am. Chem. Soc.* **1995**, *117*, 7119.
(9) (a) Murphy, C. J.; Arkin, M. A.; Jenkins, Y.; Ghatlia, N. D.; Bossman, S. H.; Turro, N. J.; Barton, J. K. *Science* **1993**, *262*, 1025. (b) Murphy, C. J.; Arkin, M. A.; Ghatlia, N. D.; Bossman, S.; Turro, N. J.; Barton, J. K. *Proc. Natl. Acad. Sci. U.S.A.* **1994**, *91*, 5315. (c) Stemp, E. D. A.; Arkin, M. R.; Barton, J. K. *J. Am. Chem. Soc.* **1995**, *117*, 2375. (d) Arkin, M. A.; Stemp, E. D. A.; Turro, C.; Turro, N. J.; Barton, J. K. *J. Am. Chem. Soc.* **1996**, *118*, 2267. (e) Arkin, M. R.; Stemp, E. D. A.; Holmlin, R. E.; Barton, J. K.; Hormann, A.; Olson, E. J. C.; Barbara, P. F. *Science* **1996**, *273*, 475.
(10) Haq, I.; Lincoln, P.; Suh, D.; Norden, B.; Chowdhry, B. Z.; Chaires, J. B. *J. Am. Chem. Soc.* **1995**, *117*, 4788.
(11) Turro, C.; Bossmann, S. H.; Jenkins, Y.; Barton, J. K.; Turro, N. J. *J. Am. Chem. Soc.* **1995**, *117*, 9026.

S0020-1669(96)00738-0 CCC: $14.00

nucleic acid structures.[6] $[Ru(phen)_2dppz]^{2+}$ complexes bound to DNA display a biexponential decay in emission.[2] Studies of asymmetrically substituted $[Ru(phen)_2dppz]^{2+}$ derivatives,[6] differential quenching experiments using hydrophobic and polar proton transfer quenchers,[11] as well as luminescence studies using a range of nucleic acids, all support models for two intercalative geometries. In the first model, the dppz ligand may intercalate in a head-on fashion with the long axis of the dppz ligand parallel to the dyad axis of the base pair. In this orientation, both phenazine nitrogens are well protected. In the second proposed orientation, these axes may form an acute angle, maximizing stacking with the base pair and producing a canted geometry in which one side of the ligand is more exposed to solvent than the other.

An important observation has been that both Λ- and Δ-isomers bound to DNA reveal biexponential decays in emission although with considerable differences in excited state lifetimes ($\tau(\Delta)$'s > $1.5\tau(\Lambda)$'s).[9,11] However, these differences are not a function of the thermodynamics of DNA binding; both isomers must be fully bound to reveal luminescence. Instead the differences in luminescence quantum yields reflect more directly differences in *how* the two isomers intercalate within a right-handed helix.[12] Likely owing to a similar sensitivity to stacking, excited state lifetimes for the dppz complexes bound to double helical DNA of different sequences also vary substantially, despite a low apparent sequence-selectivity in binding.[6] The application of this family of complexes as diagnostic probes requires also a structural understanding of these variations.

Over the last few years, our efforts to obtain structural details concerning the interactions of octahedral transition metal complexes with DNA have intensified through the application of NMR spectroscopy.[13−17] Emerging from these studies has been substantiating evidence for (i) enantioselective DNA binding by the octahedral complexes, (ii) ligand-specific intercalation for dppz and phi complexes, and (iii) intercalative access by these metal complexes from the major groove.

Recently we reported the combined use of selective deuteration of ligands and ^{1}H NMR to establish the major groove approach of Δ-$[Ru(phen)_2dppz]^{2+}$ to the hexamer $d(GTCGAC)_2$.[15a] In this more comprehensive study, we report the first comparison of the DNA binding behavior of Λ- and Δ-$[Ru(phen)_2dppz]^{2+}$ using both ^{1}H and ^{31}P NMR. Within this context, issues of intercalation, exchange rate, sequence specificity, and the distribution of binding geometries have been explored. Some differences in binding between enantiomers are evident, but there is substantial structural evidence for intercalation by both Λ- and Δ-isomers. Slow exchange conditions permit the observation of multiple, major groove intercalative binding orientations for the Δ-isomer. Indeed, these NMR data suggest that $[Ru(phen)_2dppz]^{2+}$ enantiomers bind to the DNA helix with a population of intercalative geometries, some of which provide asymmetric protection of the dppz ligand from aqueous solvent. In this first NMR study of DNA binding by the Λ-isomer, we furthermore observe significantly broader lines compared to the bound Δ-isomer, which are indicative of differences in exchange behavior between the two intercalated enantiomers. In total, the results described here serve to support and extend earlier structural models derived from luminescence studies.

Materials and Methods

Materials and Instrumentation. Oligonucleotides were synthesized using phosphoramidite chemistry[18] on an ABI DNA synthesizer and purified by reverse phase HPLC using 50 mM triethylamine acetate and acetonitrile gradients. Purified oligonucleotides were converted to the sodium salt using CM Sephadex C-25 (Sigma). 99.96 atom % D D_2O and trimethyl phosphate (TMP) were obtained from Aldrich; sodium 3-trimethylsilyl-[2,2,3,3-D_4]propionate (TMSP) and "100%" D_2O were purchased from Cambridge Isotopes. Other chemicals and biochemicals were of the highest quality available commercially. Circular dichroism (CD) spectra were recorded on a JASCO J-500C spectropolarimeter. ^{1}H and ^{31}P NMR spectra were recorded on a Bruker AMX 500 spectrometer.

Metal Complex Syntheses. Protocols for the preparation of $[Ru(phen)_2dppz]^{2+}$ used in these studies are modifications of previous methods.[6,19] Earlier procedures involve a $[Ru(phen)_2phendione]^{2+}$ intermediate. Here the dppz ligand is prepared independently and subsequently coordinated to $[Ru(phen)_2]^{2+}$ to form the complex. All metal complexes were purified by preparative reverse phase HPLC using a 50 mM TEAA/acetonitrile gradient.

$Ru(phen)_2Cl_2$ and 5,6-phendione were synthesized as previously described.[20] Dppz was synthesized by heating 100 mg of phendione in 5 mL ethanol to reflux and then adding 1.5 equiv (80 mg) of phenylene diamine. The product precipitated after 10 additional minutes of refluxing in 60% yield.

$[Ru(phen)_2dppz]^{2+}$ was assembled by refluxing 55 mg of $Ru(phen)_2Cl_2$ with 27 mg (1.1 equiv.) of dppz in 2 mL of 50% methanol for 10 h. The cooled reaction mixture was diluted with water and filtered to remove solid impurities. The complex was then separated from soluble impurities by precipitation with NH_4PF_6. Anion exchange chromatography restores the chloride salt. Yield: 52 mg (66%).

Deuterated metal complexes were synthesized using perdeuterated-d_8 phenanthroline (CDN Isotopes, Montreal, Canada) as a starting material. $Ru(phen\text{-}d_8)_2Cl_2$ was synthesized from phenanthroline-d_8; dppz-d_6 was synthesized from the oxidation of phenanthroline-d_8 to 5,6-phendione-d_6 in DNO_3 and D_2SO_4 (Cambridge Isotopes) to minimize deuterium exchange. Subsequent condensation with *O*-phenylenediamine formed the ligand. The synthesis of the full complex proceeded as described above.

7,8-Difluoro-(dipyrido[3,2-*a*:2′,3′*c*]phenazine) was synthesized using 2-amino-4,5-difluoroaniline, which was prepared from the reduction of 2-nitro-4,5-difluoroaniline (Aldrich) with $SnCl_2$ and HCl.[21] The fluorinated metal complex was assembled using the identical protocol as that described above for the unmodified complex. UV−visible spectroscopic parameters are identical to those the unmodified complex.[6b] Chemical shift data for both the fluorinated and unmodified complex are provided below.

Enantiomer Resolution. A solution containing 8 μmol of racemic $[Ru(phen)_2dppz]^{2+}$ was loaded onto a 2.5 × 75 cm SP-25 Sephadex column primed with KCl. Enantiomers were resolved by recirculating 100 mM sodium antimonyl tartrate. Three to four passes of metal complex yield a readily visible and complete separation. The metal complex was eluted from the resin with 5 M NaCl and desalted by precipitation using NH_4PF_6. Conversion to the water soluble chloride salt was achieved using a QAE A-25 anion exchange chromatography. Circular dichroism spectroscopy was used to obtain typical Δε's at 468 nm of -26 M^{-1} cm^{-1} for the Δ isomer and $+23$ M^{-1} cm^{-1} for Λ.

(12) Barton, J. K. *Science* **1986**, *233*, 727.
(13) (a) Rehmann, J. P.; Barton, J. K. *Biochemistry* **1990**, *29*, 1701. (b) Rehmann, J. P.; Barton, J. K. *Biochemistry* **1990**, *29*, 1710.
(14) David, S. S.; Barton, J. K. *J. Am. Chem. Soc.* **1993**, *115*, 2984.
(15) (a) Dupureur, C. M.; Barton, J. K. *J. Am. Chem. Soc.* **1994**, *116*, 10286. (b) Collins, J. G.; Shields, T. P.; Barton, J. K. *J. Am. Chem. Soc.* **1994**, *116*, 9840. (c) Shields, T. P.; Barton, J. K. *Biochemistry* **1995**, *34*, 15037.
(16) Shields, T. P.; Barton, J. K. *Biochemistry* **1995**, *34*, 15049.
(17) Hudson, B. P.; Dupureur, C. M.; Barton, J. K. *J. Am. Chem. Soc.* **1995**, *117*, 9379.
(18) Caruthers, M.; Beaton, G.; Wu, J. V.; Wiesler, W. *Methods Enzymol.* **1992**, *211*, 3.
(19) Amouyal, E.; Homsi, A.; Chambron, J.-C.; Sauvage, J. P. *J. Chem. Soc., Dalton Trans.* **1990**, 1841.
(20) (a) Sullivan, B. P.; Salmon. D. J.; Meyer, T. J. *Inorg. Chem.* **1978**, *17*, 3334. (b) Yamada, M.; Tanaka, Y.; Yoshimoto, Y. *Bull. Chem. Soc. Jpn.* **1992**, *65*, 1006.
(21) Uchida, M.; Morita, S.; Chihiro, M.; Kanbe, T.; Yamasaki, K.; Yabuuchi, Y.; Nakagawa, K. *Chem. Pharm. Bull.* **1989**, *37*, 1517.

NMR Analysis. Samples were prepared from 4 mM stock solutions of duplex and metal complex in 100% D_2O. Typical samples contained 1 mM duplex, 0.75 mM metal complex, 25 mM NaCl, and 10 mM phosphate in 0.5 mL of "100%" D_2O with the pH* adjusted to 7.0. Spectra were recorded on a Bruker AMX 500 at 7 °C. Chemical shifts are relative to internal TMSP. For one-dimensional ^{1}H spectra, 128 scans were collected and Fourier transformed with exponential multiplication (LB 1). For NOESY and COSY spectra, a 2048 × 512 matrix was recorded in the time domain and zero-filled to a 2048 × 2048 matrix prior to exponential multiplication (LB 1).

^{1}H-decoupled ^{31}P spectra were collected on a Bruker AMX500 at 202 MHz under the same sample conditions used for ^{1}H NMR. Chemical shifts are relative to internal TMP. Typically 3456 scans were collected and Fourier transformed with exponential multiplication (LB 3).

Molecular Modeling. Δ-[Ru(phen)$_2$dppz]$^{2+}$ was docked with d(GTCGAC)$_2$ using InsightII software (Biosym Technologies, Inc). The binding geometries were constructed based on the correlation between upfield chemical shifts and degree of intercalation into the DNA base stack.[22]

Results

Resonance Assignments. DNA duplex assignments were based on the presence of distinct base proton (H8, H6, H5, and TMe) to sugar proton sequential NOE connectivities.[23] Spectra of the free duplex were unambiguous; assignments for bound duplex rely on observable sequential connectivities, similarities to patterns observed for free duplex, and exchange peaks observed in NOESY and ROESY[24] experiments between perturbed and unperturbed resonances. In both cases, the NOE connectivities were consistent with a B conformation throughout the length of the duplex.

Metal−ligand proton resonances in the free metal complex were assigned with a combination of approaches. ^{1}H spectra of the structurally similar [Ru(phen)$_3$]$^{2+}$ display 4,7 protons of phenanthroline at low field (near 9.0 ppm) and 3,8 protons most upfield (near 7.0 ppm); 2,9 and 5,6 resonances are located near 8.0 ppm in D_2O.[13] Free [Ru(phen)$_2$dppz]$^{2+}$ displays a similar pattern. COSY spectra were helpful in distinguishing among phenanthroline proton resonances. Dppz ligand proton resonances were distinguished from phenanthroline resonances using integration measurements and ^{1}H spectra of the selectively deuterated metal complexes. Specifically, those proton resonances of [Ru(phen)$_2$dppz]$^{2+}$ which persist in spectra of [Ru(phen-d_8)$_2$dppz]$^{2+}$ must clearly correspond to dppz ligand protons. The most distal dppz ligand protons (11′−14′) were distinguished from those protons on the proximal end of the ligand (i.e., close to the ruthenium center) by comparing spectra of [Ru(phen)$_2$dppz]$^{2+}$ and [Ru(phen-d_8)$_2$dppz]$^{2+}$ with those of [Ru(phen-d_8)$_2$(dppz-d_6)]$^{2+}$, a complex containing only four protons (11′-14′). Comparison of spectra of [Ru(phen)$_2$dppz]$^{2+}$ with [Ru(phen)$_2$(diF-dppz)]$^{2+}$ and alkylated derivatives of [Ru(phen)^{2}dppz]$^{2+}$ [6] further aided in the assignment of 11′−14′ resonances of the dppz ligand.

Assignments for the bound complex were also aided through spectra obtained for deuterated complexes and through COSY experiments. That is, resonances which are present in [Ru(phen)$_2$dppz]$^{2+}$−d(GTCGAC)$_2$ samples but absent in [Ru(phen-d_8)$_2$dppz]$^{2+}$−d(GTCGAC)$_2$ samples can be unambiguously assigned to the bound dppz ligand. This same strategy was applied to spectra of [Ru(phen-d_8)$_2$(dppz-d_6)]$^{2+}$−d(GTCGAC)$_2$ in distinguishing bound (2′,9′), (3′,8′), and (4′,7′) dppz ligand protons from the 11′−14′ protons. Further, the possible chemical shifts for intercalated metal ligand protons are restricted to within 0−1.6 ppm upfield from the location of the free metal ligand resonance.[22,25] This restriction permits the unambiguous assignment of bound [Ru(phen-d_8)$_2$dppz]$^{2+}$ resonances downfield of 8.2 ppm as 4′,7′ protons. Spectral data did not permit us to distinguish further 4′ from 7′ protons. Due to spectral overlap near 8.0 ppm, it was not possible to locate bound 11′,14′ and 12′,13′ protons of the dppz ligand directly.

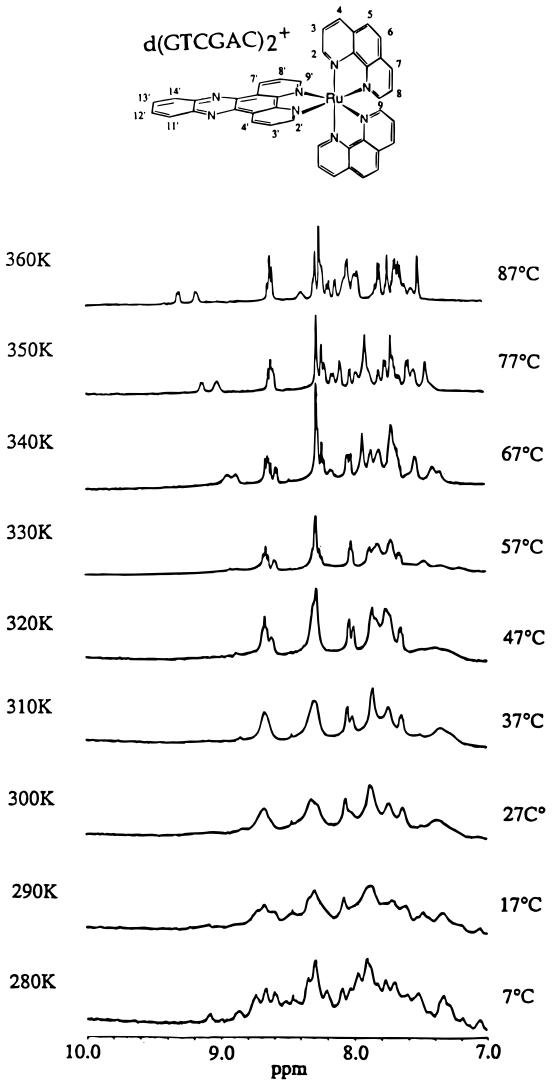

Figure 1. Variable-temperature 500 MHz ^{1}H NMR spectra of 1:1 *rac*-[Ru(phen)$_2$dppz]$^{2+}$−d(GTCGAC)$_2$ in 25 mM NaCl, 10 mM phosphate buffer, and pH* 7.0 in 100% D_2O. Chemical shifts are reported relative to TMSP (0 ppm). A schematic of the metal complex is also shown.

Estimate of Exchange Rate. Figure 1 displays the exchange behavior between *rac*-[Ru(phen)$_2$dppz]$^{2+}$ and d(GTCGAC)$_2$. As also reported by Norden and co-workers,[26] we observe intermediate exchange on the NMR time scale near ambient temperature, an exchange dynamic which is common among organic intercalators.[27] However, at temperatures near 0 °C we have been able to observe slow exchange dynamics. From the range of variable temperature data, an exchange rate of 70 s^{-1} is estimated at the coalescence temperature (300 K).[28]

(22) Giessner-Prettre, C.; Pullman, B. *Q. Rev. Biophys.* **1987**, *20*, 113.
(23) Wuthrich, K. *NMR of Proteins and Nucleic Acids;* Wiley: New York, NY, 1986.
(24) Neuhaus, D.; Williamson, M. *The Nuclear Overhauser Effect;* VCH: New York, 1989.
(25) Giessner-Prettre, C.; Pullman, B. *Biochem. Biophys. Res. Commun.* **1976**, *70*, 578.
(26) Eriksson, M.; Leijon, M.; Hiort, C.; Norden, B.; Graslund, A. *Biochemistry* **1994**, *33*, 5031.
(27) (a) Zhou, N.; James, T. L.; Shafer, R. H. *Biochemistry* **1989** *28*, 5231. (b) Searle, M. S. *Prog. NMR Spectrosc.* **1993**, *25*, 403−480.

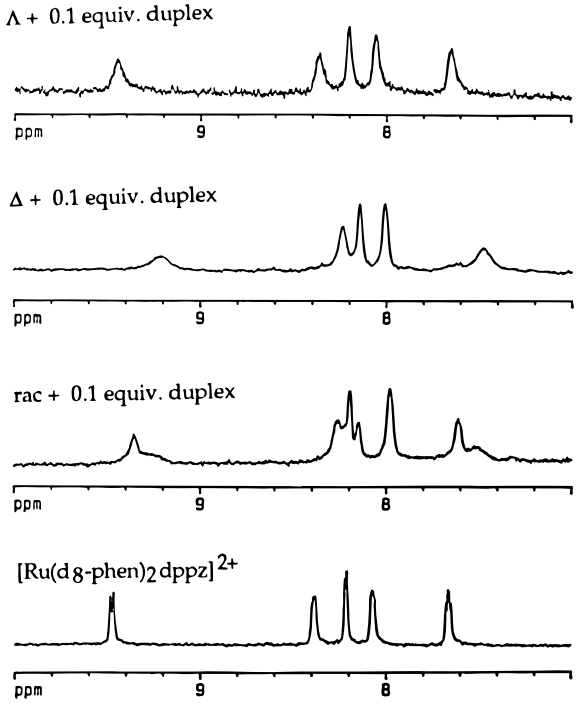

Figure 2. 500 MHz ^{1}H NMR spectra of free metal complex and *rac*-, Δ-, and Λ-[Ru(phen-d_8)$_2$dppz]$^{2+}$ in the presence of 0.1 equiv. d(GTCGAC)$_2$. Samples contained 0.5 mM metal complex, 25 mM NaCl, and 10 mM phosphate buffer, at pH* 7.0 in 100% D_2O at 280 K. Chemical shifts are reported relative to TMSP (0 ppm). Chiral shifts observed in the spectrum of bound racemic metal complex are confirmed with spectra of resolved enantiomers bound by duplex.

The achievement of slow exchange conditions is especially significant because such conditions permit the observation of individual binding orientations, instead of a less informative average among them. The ability to observe individually protons on either side of long axis of the dppz ligand provides us with a valuable level of detail about its motion and intercalative orientations.

Enantiomer Comparison using 1D ^{1}H NMR. Fundamental NMR evidence for enantioselective binding of [Ru(phen)$_2$dppz]$^{2+}$ to duplex DNA is illustrated in Figure 2 by the presence of chiral shifts in *rac*-[Ru(phen)$_2$dppz]$^{2+}$ spectra containing small amounts of duplex. A similar chiral shift difference in binding *rac*-[Ru(phen)$_3$]$^{2+}$ to a DNA hexamer has been observed.[13] The interpretation here is confirmed through spectra containing resolved enantiomers at ratios of Ru:duplex near unity (Figure 3). Although both 1D and 2D ^{1}H NMR data were collected at several metal:duplex ratios, metal complex−DNA interactions were best observed at a 0.75:1 ratio. Importantly, the downfield pattern of the 4′,7′ protons is clearly enantiospecific. For the Δ-isomer, we see four peaks ranging in upfield changes in chemical shift from −0.17 to −0.80 ppm; for the Λ-isomer, only one downfield peak is well-resolved, but there is some possibility that another exists overlapping with the A_5H8 pattern between 8.2 and 8.3 ppm. These distinct patterns point to enantioselective intercalation. Observable chemical shift changes upon binding DNA for both dppz and phenanthroline ligand protons of Λ- and δ-[Ru(phen)$_2$dppz]$^{2+}$ are compiled in Table 1. Larger perturbations (up to −0.80 ppm) are observed for the dppz ligand protons, while much smaller perturbations (<0.3 ppm) are observed for the ancillary phenanthroline ligands. This behavior is consistent with the dppz ligand preferentially participating in stacking with d(GTCGAC)$_2$ and is reminiscent of that observed for [Rh(phen)$_2$phi]$^{3+}$ upon binding DNA.[14] The magnitude and direction of the chemical shift changes for the dppz ligand protons[15,29] are indicative of selective intercalation of this ligand by both enantiomers. This interpretation is entirely consistent with earlier luminescence results.[2,6−7,11]

Importantly, differences in binding by the enantiomers are evident not only in resonance positions but also in exchange dynamics. In the 1D spectra of Λ- and δ-[Ru(phen-d_8)$_2$dppz]$^{2+}$ bound to d(GTCGAC)$_2$ shown in Figure 3, a difference in line width is immediately apparent. Broader lines in spectra for λ-[Ru(phen-d_8)$_2$dppz]$^{2+}$ may be attributed either to a reduced binding specificity compared to the Δ-isomer and/or a somewhat faster exchange rate.

Intermolecular NOEs. Δ-[Ru(phen)$_2$dppz]$^{2+}$. For the Δ-isomer bound to DNA, intermolecular NOEs are evident, reproducible, and persist at low mixing times. Selective deuteration was used to assign the intermolecular NOE observed in Figure 3 between an H2′2″ sugar proton of the duplex and 2′,9′ protons of the dppz ligand of Δ-[Ru(phen)$_2$dppz]$^{2+}$. Given this close contact between a sugar proton and these dppz protons near the metal center, this intermolecular NOE is fully consistent with an intimate interaction.[23] Although this NOE cannot be unambiguously assigned to a particular residue or even as a major or minor groove contact,[30] the observed NOE is certainly consistent with intercalation.

We also observe, as previously reported,[15] two intermolecular NOEs between the highly shifted A_5H8 and two peaks (8.82 and 8.58 ppm) assigned to the 4′,7′ protons of the dppz ligand of Δ-[Ru(phen)$_2$dppz]$^{2+}$. These are indicated for the Δ-isomer but not the Λ-isomer bound to DNA in Figure 3. The geometry of the dppz ligand and the location of A_5H8 in the helix preclude NOEs to both 4′ and 7′ protons of the same bound complex simultaneously. Hence, the two NOEs to this DNA proton would indicate at least *two* major groove binding orientations for the metal complex intercalated into the helix.

The strength of these intermolecular NOEs suggested the possibility that A_5H8 and a metal−ligand proton resonance might be overlapping. Importantly, however, the line shape of this peak was not affected by the substitution of metal ligand protons through deuteration. Additionally, exchange peaks between this peak and other A_5H8 resonances were visible in ROESY spectra. Thus the assignment of an intermolecular NOE between A_5H8 and proximal dppz protons remains sound, and the observation therefore establishes multiple major groove binding orientations for Δ-[Ru(phen)$_2$dppz]$^{2+}$.

No intermolecular NOEs between the oligonucleotide and the phenanthroline ligands of [Ru(phen)$_2$dppz]$^{2+}$ could be assigned at either 500 or 600 MHz field strength (data not shown). On the basis of molecular modeling, the length of the dppz ligand may place these ancillary ligand protons out of reach of nonexchangeable DNA protons.

Λ-[Ru(phen)$_2$dppz]$^{2+}$. In contrast to results found for the Δ-isomer, no intermolecular NOEs between the oligonucleotide and Λ-[Ru(phen)$_2$dppz]$^{2+}$ protons could be assigned in any portion of NOESY spectra (Figure 3). The line widths in these spectra are likely responsible for this observation. However, NOESY cross-peak patterns in the diagnostic H2′2″ region for d(GTGCAC)$_2$ bound by Λ- and Δ-[Ru(phen)$_2$dppz]$^{2+}$ may be compared. The pattern is quite similar between the enantiomers, with the peak patterns near 7.0 ppm representing subtle

(28) Fede, A.; Labhardt, A.; Bannwarth, W.; Leupin, W. *Biochemistry* **1991**, *30*, 11377.

(29) Feigon, J.; Denny, W. A.; Leupin, W.; Kearns, D. R. *J. Med. Chem.* **1984**, 450.

(30) (a) Leonard, G. A.; Hambley, T. W.; Mcauleyhecht, K.; Brown, T.; Hunter, W. N. *Acta Crystallogr., Sect. D* **1993** *49*, 458. (b) Smith, C. K.; Davies, G. J.; Dodson. E. J.; Moore, M. H. *Biochemistry* **1995**, *34*, 415.

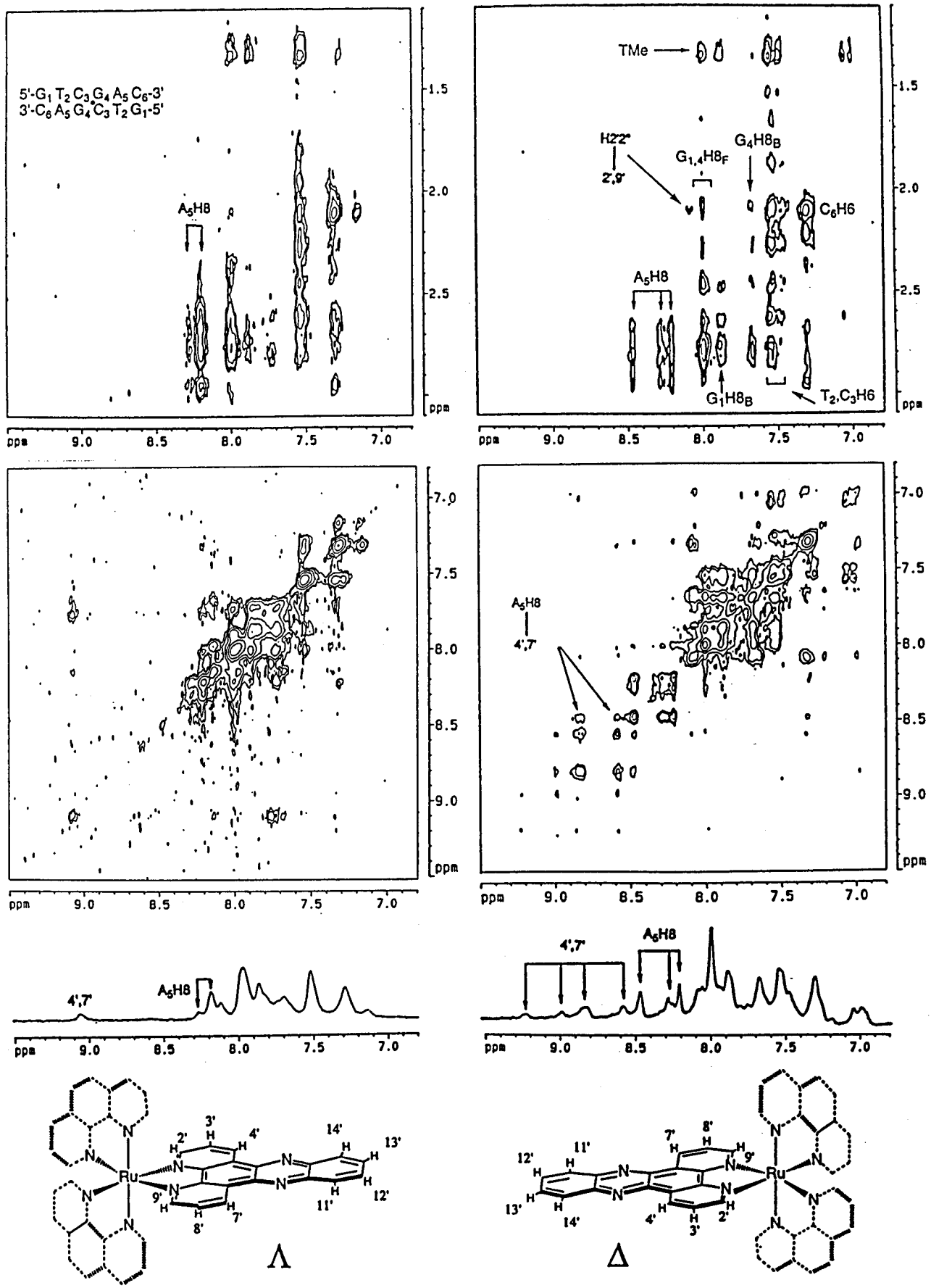

Figure 3. Comparison of enantiomeric DNA binding behavior of [Ru(phen-d_8)$_2$dppz]$^{2+}$ by ^{1}H NMR. Depicted are schematics of the deuterated enantiomers, the aromatic regions of one-dimensional spectra, and the aromatic−aromatic and base-H2′H2″ regions of two-dimensional NOESY spectra of Λ- and Δ-[Ru(phen-d_8)$_2$dppz]$^{2+}$ bound by d(GTCGAC)$_2$. Samples contained 0.75:1 metal complex−duplex, 1 mM duplex, 25 mM NaCl, and 10 mM phosphate buffer, at pH* 7.0 in 100% D_2O at 280 K. Chemical shifts are reported relative to TMSP (0 ppm). Spectra were collected at 500 MHz. The mixing time for NOESY experiments was 300 ms. Resonance assignments and intermolecular NOEs (A_5H8-4′,7′ and H2′2″-2′,9′) are indicated. "B" denotes bound or perturbed resonances; "F" denotes free or unperturbed resonances.

Table 1. Chemical Shift Data for Λ- and Δ-$[Ru(phen)_2dppz]^{2+}$ Bound to $d(GTCGAC)_2$

	Δ-isomer			Λ-isomer	
proton	δ(free), ppm	δ(bound), ppm	Δ(δ), ppm	δ(bound), ppm	Δ(δ), ppm
2′,9′-dppz	8.21	7.87	−0.34	8.14	−0.07
		8.07	−0.14	(8.21)[a]	0.00
				(8.11)	−0.10
3′,8′-dppz	7.70	6.99	−0.71	7.79	0.09
		7.33	−0.37	7.32	−0.38
		7.52	−0.18		
		7.61	−0.09		
4′,7′-dppz	9.38	8.58	−0.80	9.08	−0.30
		8.82	−0.56		
		8.98	−0.40		
		9.21	−0.17		
2,9-phen	8.13	(8.28)	0.15	8.08	−0.05
	8.36		−0.08	8.38	0.02
3,8-phen	7.62	7.97	0.35	7.84	0.22
		7.92	0.30	7.58	−0.04
		7.77	0.15		
		7.72	0.10		
		7.70	0.08		
4,7-phen	8.62	8.73	0.11	8.62	0.00
		8.70	0.08	8.59	−0.03
		8.67	0.05		
		8.62	0.00		
5,6-phen	8.27	(8.35)	0.08	na[b]	...

[a] Tentative assignments are shown in parentheses. [b] na = not assigned. [c] Bound chemical shifts for 11′,14′ and 12′,13′ protons could not be unambiguously assigned due to spectral overlap.

differences. The most prominent difference between the spectra lies in the A_5H8 patterns. The highly downfield shifted A_5H8 observed with Δ-$[Ru(phen)_2dppz]^{2+}$ is absent in spectra with the Λ-isomer. Thus the accompanying intermolecular NOE is absent, establishing this particular major groove contact for the Δ-isomer as enantioselective. No evidence for a major groove orientation for the Λ-isomer is therefore provided in these spectra.

Pattern of Intercalated Δ-$[Ru(phen)_2dppz]^{2+}$ Ligand Protons. Slow exchange conditions permitted the observation of a range of chemical shifts for the 3′,8′ and 4′,7′ resonances of the dppz ligand of Δ-$[Ru(phen)_2dppz]^{2+}$. From Figure 3, it is clear that the 4′,7′ resonance at 8.8 ppm is 2−3 times the size of the others. Thus at least two but possibly more binding orientations are represented in this pattern. Both must be intercalative given the magnitude of the upfield changes in chemical shift. It was not possible to "pair" 4′ with corresponding 7′ resonances for each binding orientation, however. These protons are not only exchanging with each other (a 180° flip about the long axis of the dppz ligand exchanges the location of these two protons with one another), but with other binding orientations as well. It is evident nonetheless that intercalation into the helix renders these protons inequivalent. Coupled with the range in upfield changes in chemical shift for these protons, a distribution of canted geometries is an attractive explanation for this pattern.

Quantitative DNA Perturbations by Δ-$[Ru(phen)_2dppz]^{2+}$. Chemical shift changes for DNA protons that have been identified in the form bound by Δ-$[Ru(phen)_2dppz]^{2+}$ are summarized in Table 2. In the analysis of these data, it is first helpful to recall that one metal complex asymmetrically bound with respect to the duplex can produce two resonances for each DNA proton in a self-complementary duplex: one highly perturbed proton, and one less perturbed resonance, which may lie very near its chemical shift in the free duplex. The result is a spectrum which contains about twice as many resonances,

Table 2. Summary of DNA Chemical Shift (ppm) Perturbation by Δ-$[Ru(phen)_2(dppz)]^{2+}$

residue		BH6/8	H5-Me	H1′	H2′	H2″
G_1	free	8.02		6.06	2.85	2.77
	bound	7.87		6.04	2.48	2.76
					2.64	
	Δδ	−0.15		−0.02		
T_2	free	7.58	1.36	6.22	2.28	2.62
	bound	7.52,7.03	1.33	(5.89)[a]	2.25	2.62
	Δδ	−0.06, −0.55	−0.33	(−0.33)	−0.03	0.00
C_3	free	7.53	5.68	5.69	2.06	2.45
	bound	7.46	5.87	5.68	2.08	2.46
	Δδ	−0.07	0.19	−0.01	0.02	−0.01
G_4	free	8.01		5.63	2.82	2.82
	bound	7.69		5.61	na[b]	na[b]
	Δδ	−0.32		−0.02	...	...
A_5	free	8.22		6.31	2.68	2.95
	bound	8.46, 8.28		na[b]	2.69	2.96
	Δδ	0.24		...	0.01	0.01
C_6	free	7.32	5.30	6.06	(2.11)	(2.11)
	bound	7.26, 7.03	5.56	na[b]	na[b]	(2.09)
	Δδ	−0.06 −0.29	0.24	...	...	(−0.02)

[a] Tentative assignments are shown in parentheses. [b] na = not assigned. [c] It was not possible to assign resonances for bound A_5H2, H3′ and H4′ protons.

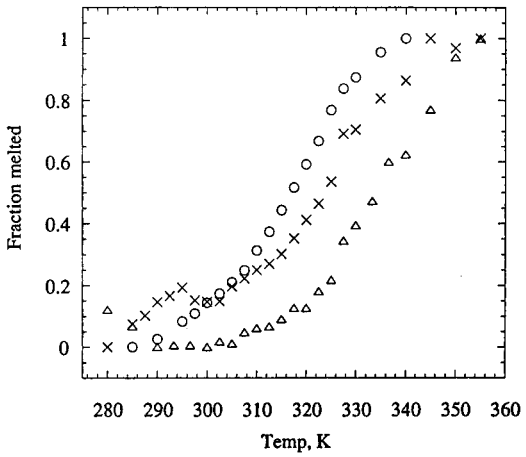

Figure 4. Melting curves for $d(GTCGAC)_2$ unbound (○) and in the presence of Λ-$[Ru(phen)_2dppz]^{2+}$ (×) and Δ-$[Ru(phen)_2dppz]^{2+}$ (△).

half of which may exhibit patterns quite similar to those observed for the free duplex.

Asymmetry in binding by the metal complex *with respect to the DNA* is immediately evident through the presence of nondegenerate base protons in the H2′2″ region (A_5H8, G_1H8, G_4H8, and T_2H6); shifted C_3 and C_6 protons are evident in the H5/6 region (5.0−5.5 ppm) of spectra of $d(GTCGAC)_2$ bound by Δ-$[Ru(phen)_2dppz]^{2+}$ (see Supporting Information). Since there is only one A per strand, the presence of three A_5H8 resonances necessitates more than one asymmetric binding interaction with the metal complex. Prominent perturbations include the +0.24 ppm shifted A_5H8 and the −0.33 ppm shifted T_2H6. These data indicate that the metal complex does not intercalate in the central 5′-CG-3′ step, but rather in one or both of the two remaining base steps.

Duplex Melting Behavior. Enantioselectivity is also apparent as a function of melting the helix. Figure 4 summarizes the melting behavior of $d(GTCGAC)_2$ alone and in the presence of Λ- and Δ-$[Ru(phen)_2dppz]^{2+}$. Data points were derived from variable temperature ^{1}H chemical shift information on free duplex and 1:1 Ru−duplex samples. The melting temperature

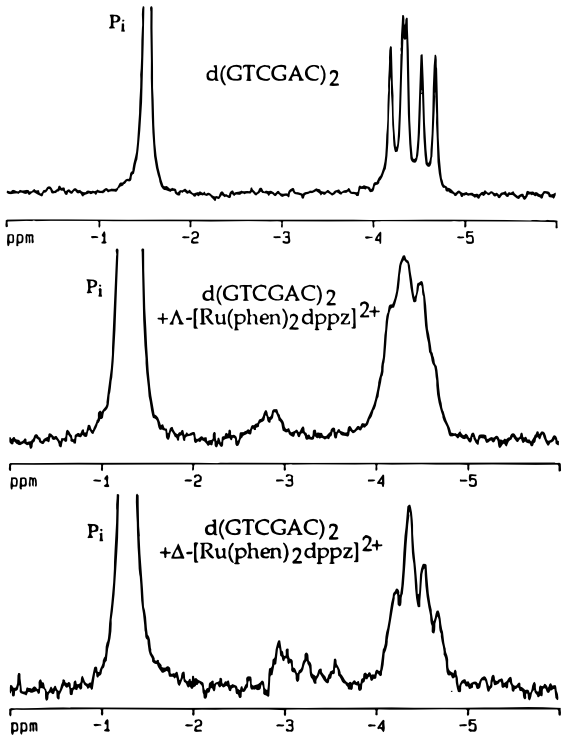

Figure 5. 202 MHz ^{31}P NMR spectra of d(GTCGAC)$_2$ unbound and in the presence of Λ-[Ru(phen)$_2$dppz]$^{2+}$ and Δ-[Ru(phen)$_2$dppz]$^{2+}$. Samples contained 0.75:1 metal complex−duplex, 1 mM duplex, 25 mM NaCl, and 10 mM phosphate buffer, at pH* 7.0 in 100% D_2O at 280 K. Chemical shifts are reported relative to trimethyl phosphate (0 ppm).

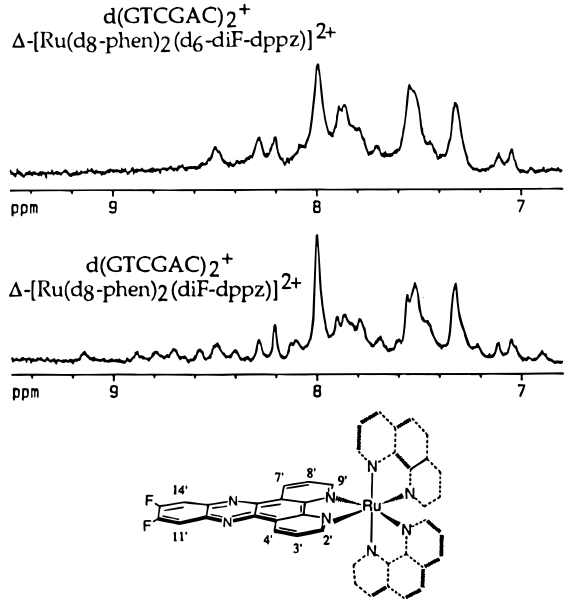

Figure 6. 500 MHz ^{1}H NMR spectra of d(GTCGAC)$_2$ bound by 0.75 equiv of Δ-[Ru(phen-d_8)$_2$(diF-dppz)]$^{2+}$ and Δ-[Ru(phen-d_8)$_2$(d$_6$-diF-dppz)]$^{2+}$. Samples contained 1 mM duplex, 0.75 mM metal complex, 25 mM NaCl, and 10 mM phosphate buffer, at pH* 7.0 in 100% D_2O at 280 K. Chemical shifts are reported relative to TMSP (0 ppm). A schematic of Δ-[Ru(phen-d_8)$_2$(diF-dppz)]$^{2+}$ is shown. Resonances for 4′,7′ protons are readily identified through comparison of the deuterated forms of the complex. Note the distinct patterns of these resonances for the fluorinated complex compared to those observed with the unmodified complex (Figure 3), indicating different intercalative geometries.

of the free duplex (T_m) is 318 K. In the presence of Λ-[Ru(phen)$_2$dppz]$^{2+}$, it increases modestly to 323 K (ΔT_m = 5 °C); with Δ-[Ru(phen)$_2$dppz]$^{2+}$, the melting temperature is 334 K (ΔT_m = 16 °C). The observation that both isomers increase the T_m is consistent with that expected for intercalators and indicates stabilization by the metal complex of the double helix over the single-stranded form.[31] The Δ-isomer improves the helical stability of the right-handed duplex to a greater extent than does the Λ-isomer. A small difference in stabilization by the two isomers has also been observed by calorimetry.[10]

^{31}P Phosphorus NMR. ^{31}P NMR studies of oligonucleotides bound by intercalators provide direct information concerning any backbone distortions which accompany the interaction.[32] As shown in Figure 5, the free oligonucleotide exhibits a collection of resonances near −4 ppm, a chemical shift typical for B form DNA; all five phosphates are individually resolved. When the oligonucleotide is bound by either enantiomer of [Ru(phen)$_2$dppz]$^{2+}$, intensity 1−2 ppm downfield of the free signal is evident. Unlike ^{1}H nuclei, for which upfield movement of ligand resonances is caused by increases in shielding due to penetration into the ring currents of the base stack, the movement of ^{31}P nuclei in oligonucleotides is governed by changes in the torsion angles about the phosphodiester linkage. Downfield shifts are consistent with a B_{II} conformation; this geometry better accommodates intercalators. Both the degree and direction of the shift we observe for the duplex in the presence of both enantiomers are fully consistent with what is observed for oligonucleotides bound by organic intercalators.[33] The resonances representing the bound duplex are quite broad. Since it is necessary in correlated spectroscopy for the line widths to be narrower than the coupling constants, assignment of the bound ^{31}P signals by this method was not feasible.

Fluorinated Derivatives of [Ru(phen)$_2$dppz]$^{2+}$. Our interest in understanding the details of intercalation prompted us also to examine how modifications to the intercalating ligand change stacking geometries. Our laboratory has been successful in modulating recognition behavior of metallointercalators by altering ancillary ligand structure. Derivatized phenylenediamines provide a facile synthetic route to dppz ligands which feature substitutions on the distal (or phenazine) portion of the ligand (positions 11′-14′).[6] Studies of oligonucleotide interactions involving these modified metal complexes allow us to probe the influence of this portion of the ligand on intercalative geometry. To illustrate this strategy, [Ru(phen)$_2$(diF-dppz)]$^{2+}$, a derivative featuring two fluorine substitutions for the 12′ and 13′ hydrogens, was prepared. Selective deuteration and ^{1}H NMR spectroscopy were used to evaluate the effects of this modest substitution on the geometry of intercalation.

Deuteration of the phen ligands permits the clear observation of the bound 4′,7′ protons of both unmodified and fluorinated forms of the dppz ligand. 2D NOESY spectroscopy using Δ-[Ru(phen-d_8)$_2$(dppz-d_6)]$^{2+}$ distinguish these resonances from DNA resonances (usually AH8). Figure 6 displays this aromatic region of 1D spectra of deuterated forms of Δ-[Ru(phen)$_2$(diF-dppz)]$^{2+}$ bound to the oligonucleotide. Table 3 summarizes the chemical shift behavior for the dppz ligands of these complexes. Four 4′,7′ resonances are observed for the unmodified complex, with $\Delta\delta$'s ranging from −0.17 to −0.80 ppm. Interestingly, six such peaks are visible for the fluorinated complex, with a range of chemical shift change of −0.42 to −1.16 ppm relative to the free complex in buffer. Since the magnitude of change

(31) (a) Kumar, C. V.; Asuncion, E. H. *J. Am. Chem. Soc.* **1993**, *115*, 8547. (b) Tarui, M.; Doi, M.; Ishida, T.; Inoue, M.; Nakaike, S.; Kitamura, K. *Biochem. J.* **1994**, *304*, 271.
(32) Gorenstein, D. G. *Methods Enzymol.* **1992**, *211*, 254.
(33) (a) Searle, M.; Bicknell, W. *Eur. J. Biochem.* **1992**, *205*, 45. (b) Brown, D. R.; Kurz, M.; Kearns, D. R.; Hsu, V. L. *Biochemistry* **1994**, *33*, 651.

Table 3. Chemical Shifts (ppm) for the 4′,7′-dppz Protons in Δ-[Ru(phen)$_2$dppz]$^{2+}$ and Δ-[Ru(phen)$_2$(diF-dppz)]$^{2+}$ Bound by d(GTCGAC)$_2$

δ(free)	δ(bd Δ)	Δ(δ Δ)	δ(free diF)	δ(bd ΔdiF)	Δδ(ΔdiF)
9.38	8.58	−0.80	9.56	8.40	−1.16
	8.82	−0.56		8.58	−0.98
	8.98	−0.40		8.65	−0.92
	9.21	−0.17		8.79	−0.77
				8.88	−0.68
				9.15	−0.42

in chemical shift upon intercalation is correlated with the degree of penetration into the base stack,[22,25] it follows that Δ-[Ru(phen)$_2$(diF-dppz)]$^{2+}$ is a somewhat better intercalator, i.e., stacked more deeply into the helix. While the distribution of resonances is altered at least somewhat by inherent differences in chemical shift of ligand protons due to the presence of the fluorines, the difference in chemical shift *changes* suggest that some small adjustments in intercalative geometry have also occurred to better accommodate the substitution. Luminescence studies of Δ-[Ru(phen)$_2$(diF-dppz)]$^{2+}$ bound to DNA are consistent with this notion. A small decrease in luminescense intensity for the DNA-bound form with fluorine substitution is observed as is an increase in proportion of the long-lived component (that assigned to the head-on mode).

2D NOESY data (not shown) indicate that perturbations to the DNA by both enantiomers are quite similar to those observed with unmodified complex, although the prominent 4′,7′-A$_5$H8 intermolecular NOEs observed with unmodified Δ-[Ru(phen)$_2$dppz]$^{2+}$ are lost. Spectral patterns for Λ-[Ru(phen)$_2$(diF-dppz)]$^{2+}$ and Λ-[Ru(phen)$_2$dppz]$^{2+}$ bound to d(GTCGAC)$_2$ were virtually indistinguishable.

Discussion

We have undertaken a multifaceted NMR study which probes the structural details of the interactions between the enantiomers of Λ- and Δ-[Ru(phen)$_2$(dppz)]$^{2+}$ and oligonucleotide DNA. Our interest is in placing the extensive luminescence data for these nonspecific DNA intercalators in some structural context. This work has offered at least two important challenges. First, it is important to characterize the DNA stacking, which is intrinsic to the dppz complexes despite their apparent sequence neutrality, to apply the complexes usefully both as probes of DNA and, in particular, as probes of electron transfer reactions mediated by DNA. The construction of other metallointercalators which contain a variety of ancillary ligands to attain sequence-specificity has been accomplished and sequence-specific intercalation has been characterized at high resolution using NMR methods.[17] In such metal-DNA complexes, however, the stacking orientations are likely governed by the sequence-specific contacts. For the sequence-neutral dppz complexes, in contrast, the stacking orientations should depend primarily on dppz intercalation. Given the general sequence-neutrality of the dppz complexes, a detailed DNA-bound structure determination via NMR is not feasible. We may, however, apply a range of NMR methods to examine binding to a hexamer oligonucleotide, in which binding sites for the metal complex are minimized, to address important issues of intercalative geometry, exchange, and fundamental differences in binding characteristics of enantiomers.

Second, the wealth of overlapping aromatic protons on these octahedral complexes which contain polypyridyl chelate ligands offers a challenge with respect to analysis. The application of selective deuteration of metal complex ligands in the identification of bound ligand protons was therefore essential.[34] The unbound metal complex contains 26 aromatic protons; due to the C_2 symmetry of the complex, 13 separate signals are observed. Slow exchange conditions gave rise to the observation of multiple bound forms, further compounding the assignment problem. Ligand-selective deuteration has permitted the facile distinction of dppz protons from phenanthroline protons and 2′,9′, 3′,8′, and 4′,7′ protons from 11′−14′ protons on the dppz ligand and hence our ability to focus in detail on the stacking characteristics of the DNA-bound dppz ligand.

Comparison of Exchange Rates among Octahedral Metallointercalators. At an estimated rate of 70 s^{-1}, [Ru(phen)$_2$dppz]$^{2+}$ exchanges with DNA at a much slower rate (at least an order of magnitude) that its parent molecule [Ru(phen)$_3$]$^{2+}$, for which slow exchange is not accessible under solution conditions.[13] This rate is comparable to that observed for [Rh(phen)$_2$phi]$^{3+}$ [14] and somewhat faster than what we observe for [Rh(phi)]$^{3+}$ complexes with aliphatic ligands.[15,16] For these latter complexes, of which Δ-α-[Rh[(*R*,*R*)-Me$_2$trien]phi]$^{3+}$ is the best example,[16] slow exchange with oligonucleotide DNA is observed at room temperature. A qualitative order of decreasing exchange rate with oligonucleotide DNA among octahedral transition metal complexes examined is as follows: [Ru(phen)$_3$]$^{2+}$ >> [Rh(phen)$_2$phi]$^{3+}$ > [Ru(phen)$_2$dppz]$^{2+}$ > [Rh(en)$_2$phi]$^{3+}$ > [Rh(NH$_3$)$_4$phi]$^{3+}$ > Δ-α-[Rh[(*R*,*R*)-Me$_2$trien]phi]$^{3+}$. From this trend it is evident that increasing the surface area for intercalation (dppz > phi > phen) slows down the rate of exchange of the metallointercalator. This hierarchy also indicates generally slower exchange among the aliphatic [Rh(phi)]$^{3+}$ complexes, which may arise due to the deep intercalation afforded with the smaller ancillary ligands; complexes with bulkier ancillary ligands would not be able to penetrate the base stack as deeply and thus would exchange faster.

Contrast of Enantiomeric Behavior. A variety of studies using techniques ranging from photophysics to photocleavage has focused on the binding of Δ-isomers to right-handed DNA. We have observed repeatedly that with ancillary ligands such as phenanthroline, which can span the helical groove of DNA, Δ-isomers bind more tightly by intercalation to right-handed duplexes than do Λ-isomers,[12] and enantioselectivity correlates directly with the steric bulk of the ancillary ligands.[16,35] With phenanthrolines in the ancillary positions, spanning a distance which is comparable to the DNA groove, the thermodynamic preference is small.[1,36] For [Ru(phen)$_2$dppz]$^{2+}$ enantiomers bound to calf thymus DNA, the preference for the Δ-isomer is ∼ 1 kcal.[10] Yet, DNA-bound Λ-isomers of [Ru(dppz)]$^{2+}$ luminesce with significantly shorter excited state lifetimes than bound Δ-isomers.[6,11] This observation is attributed to the poorer fit of the left-handed complex into the right-handed helix, making the phenazine nitrogens of the dppz ligand more accessible to water. NMR spectroscopy provides a unique opportunity *structurally* to examine and compare both enantiomers bound to duplex DNA.

NMR spectra of Λ-[Ru(phen)$_2$dppz]$^{2+}$−d(GTCGAC)$_2$ feature broader lines and smaller signal-to-noise ratios than do spectra of the Δ-isomer bound to DNA. It is interesting that the same characteristic observation is made in comparing NMR spectra of complexes of [Rh(phen)$_2$phi]$^{3+}$ [37] or [Rh(en)$_2$phi]$^{3+}$ [15] bound to oligonucleotides. This trend results from either a difference

(34) Thummel, R. P.; Williamson, D.; Hery, C. *Inorg. Chem.* **1993**, *32*, 1587.
(35) (a) Sitlani, A.; Barton, J. K. *Biochemistry* **1994**, *33*, 12100. (b) Sitlani, A.; Dupureur, C. M.; Barton, J. K. *J. Am. Chem. Soc.* **1993**, *115*, 12589.
(36) (a) Barton, J. K.; Goldberg, J. M.; Kumar, C. V.; Turro, J. K. *J. Am. Chem. Soc.* **1986**, *108*, 2081. (b) Campisi, D.; Morii, T.; Barton, J. K. *Biochemistry* **1994**, *33*, 4130.
(37) Dupureur, C. M.; Barton, J. K. Unpublished results.

in exchange rate between Δ and Λ octahedral complexes and/or differences in specificity of binding. The consistently poorer resolution observed in DNA-bound spectra containing Λ-isomers is in itself a general indication of the poorer fit of the left-handed isomers into the right-handed helix, the basis for enantioselectivity in binding to right-handed DNA by these chiral complexes.[12]

Despite the lower resolution of spectra for the Λ-isomer, some specific information regarding binding mode and orientations is available. Importantly, the upfield changes in chemical shift for the protons of the dppz ligand upon binding the oligonucleotide are indicative of appreciable intercalation for both enantiomers. Increases in melting temperature (T_m) seen here for both isomers further support helix stabilization on binding. Increases observed are comparable to those observed for duplexes bound by organic intercalators[31] and have been observed also for an achiral dppz complex of ruthenium.[38]

^{31}P NMR results add additional support for intercalation by both isomers. Perturbations in ^{31}P NMR chemical shift on DNA binding are comparable in direction and magnitude to those found for classical intercalators.[32,33] Indeed, these spectra represent the first characterization of intercalation by any octahedral metal complexes using ^{31}P NMR spectroscopy and serve to confirm, once again, the similarity in modes of DNA association by synthetic octahedral complexes and organic natural product intercalators.

Although it is apparent then that Λ-Ru(phen)$_2$dppz^{2+}, like the Δ-isomer, binds DNA by intercalation, significantly larger perturbations are evident with the Δ-isomer, both with respect to T_m's and the resolution of ^{1}H and ^{31}P resonances. What can we therefore discern regarding differences in geometries for intercalation between enantiomers? Here, information is available directly from spectra of Λ- and Δ-[Ru(phen)$_2$dppz]$^{2+}$ in the presence of d(GTCGAC)$_2$. The difference in the 4′,7′ resonance patterns between the enantiomers is distinct, a clear indication that the dppz ligand of each enantiomer samples a different set of angles with respect to the base pair dyad axis. Furthermore, just as we see with respect to the luminescence data,[6,11] the relative proportions of different intercalative binding geometries, as judged by the relative intensities of symmetric and asymmetrically shifted 4′,7′ resonances, differ for the two enantiomers. Both isomers intercalate, but the orientations for intercalative stacking vary between the isomers and must be sensitive to ancillary ligand disposition.

Sequence Specificity. There is very little preexisting information about the sequence specificity of [Ru(phen)$_2$dppz]$^{2+}$.[6] Sequence specificity is best determined in experiments where a DNA cleaving moiety is either incorporated or appended onto the DNA-binding molecule. [Rh(phi)]$^{3+}$ complexes, for example, promote direct strand cleavage with photoactivation.[39] In contrast, the photochemistry of ruthenium(II) polypyridyls, which targets guanines through singlet oxygen chemistry,[40] is not suitable for use as a high resolution site-selective probe of metal complex specificity. Furthermore, within the context of a small oligonucleotide, we can draw few conclusions regarding site preferences using NMR.

In contrast to results observed for oligonucleotide interactions with [Rh(phen)$_2$phi]$^{3+}$ (in fast exchange)[14] and Δ-α-[Rh[(*R*,*R*)-Me$_2$trien]phi]$^{3+}$ (in slow exchange),[17] significant interruptions in sequential base-to-sugar NOE connectivities are not evident in duplex DNA bound by Δ-[Ru(phen)$_2$dppz]$^{2+}$. There are several explanations for this, any of which may be operating in concert: (i) The exchange dynamic, with its inherent line width relationship, simply does not afford sufficient signal to noise ratios. (ii) In slow exchange, the asymmetric binding of the metal complex destroys the C_2 symmetry of the self-complementary duplex, and thus the overall intensity of the peaks used in following sequential connectivities is less, thus affecting resolution. (iii) [Ru(phen)$_2$dppz]$^{2+}$ simply binds DNA less specifically than either of the [Rh(phi)]$^{3+}$ complexes. The combination of slow exchange kinetics, evidence for intercalation, and the lack of sequential connectivity information certainly suggests a relatively low level of sequence selectivity. It also follows, then, that a lack sequence connectivity disruption cannot be taken as evidence for nonintercalative binding.

The observation of a few specific intermolecular NOEs between Δ-[Ru(phen)$_2$dppz]$^{2+}$ and the oligonucleotide(s) suggests however that some binding preferences are expressed for certain base steps of the oligonucleotide under NMR conditions. The fact that we can see specific NOEs at mixing times of 300 ms and 150 ms represents an improvement in specificity and exchange compared to [Ru(phen)$_3$]$^{2+}$, for which mixing times on the order of 400 ms were needed to observe intermolecular contacts.[26,41] The NOEs observed here to A_5H8 place two significantly populated binding sites on either side of A_5, that is, between G_4 and A_5 and/or between A_5 and C_6. Detection of a highly shifted T_2H6 is also consistent with this binding preference. The data do not permit us to distinguish multiple binding orientations within one base step from binding on either site of a base pair, however. The presence of G_4 sugar sequential connectivities to shifted (and therefore) *bound* A_5H8 base resonances suggests that the preferred site may be between A_5 and C_6. Luminescence studies have shown a preference for Δ-[Ru(phen)$_2$dppz]$^{2+}$ in binding to poly dAT compared to poly dGC and photocleavage experiments based upon singlet oxygen sensitization also indicate some sequence preferences in binding to oligonucleotides.[42] The quality of spectra of Λ-[Ru(phen)$_2$-dppz]$^{2+}$−d(GTCGAC)$_2$ precludes any comments on binding preferences for this isomer.

Intermolecular Contacts. Despite the potential for contact between the DNA and the phenanthroline ligands of [Ru(phen)$_2$dppz]$^{2+}$, no such intermolecular NOEs were evident (we cannot preclude such contacts obscured in the very crowded region near 8 ppm, however). It is interesting that both with Λ- and with Δ-[Rh(phen)$_2$phi]$^{3+}$, a multitude of such contacts are visible, even under slow exchange conditions.[14,37] To a first approximation, this contrast illustrates quite dramatically the effect of the intercalating ligand on metal complex binding behavior, even when the ancillary ligands are identical (phenanthroline in each case) and the metal centers (Ru^{2+} vs Rh^{3+}) are essentially the same size. The longer dppz ligand may lead to more canted geometries for intercalation so as to maximize stacking. Such a binding geometry would put the phenanthrolines further away from the grooves of the DNA, where the potential for DNA contact is reduced. Another possibility is that the metal complex is sampling a collection of related intercalative geometries which produce small but detectable changes in the angle between the long axis of the dppz ligand and the dyad axis of the base pair. These movements require the phenanthroline ligands to sweep through a significantly larger amount of space. If the phenanthroline ligands spend little time in any one location in space, then there is also little

(38) Neyhart, G. A.; Grover, N.; Smith, S. R.; Kalsbeck, W. A.; Fairley, T. A.; Cory, M.; Thorp, H. H. *J. Am. Chem. Soc.* **1993**, *115*, 4423.
(39) Sitlani, A.; Long, E. C.; Pyle, A. M.; Barton, J. K. *J. Am. Chem. Soc.* **1992**, *114*, 2303.
(40) Mei, H. Y.; Barton, J. K. *Proc. Natl. Acad. Sci. U.S.A.* **1988**, *85*, 1339.
(41) Eriksson, M.; Leijon, M.; Hiort, C.; Norden, B.; Graslund, A. *J. Am. Chem. Soc.* **1992**, *114*, 4933.
(42) Arkin, M. R.; Stemp, E. D. A.; Barton, J. K. Submitted for publication.

time for NOE buildup. Molecular modeling additionally suggests that DNA contact with the phenanthroline ligands might be more likely with exchangeable imino protons than with the nonexchangeable protons observed in this study. While 1D studies in 90% H_2O/10% D_2O clearly demonstrated upfield shifts and broadening of imino protons upon binding of the metal complex (see Supporting Information), line widths in the [Ru(phen)$_2$dppz]$^{2+}$−d(GTCGAC)$_2$ system preclude high-resolution two-dimensional studies under 90/10 H_2O/D_2O conditions.

Intercalative Major Groove Binding Orientations. While the major groove approach of [Rh(phi)]$^{3+}$ complexes has been established for some time,[14,17,37,43] the groove preference for the structurally similar [Ru(phen)$_2$dppz]$^{2+}$ has been more elusive. NMR studies have demonstrated that there are at least two major groove binding orientations for the Δ-isomer.[15a] This result is derived from the pattern of bound 4′,7′ protons of the dppz ligand and accompanying NOEs to the major groove proton AH8.

Since upfield changes in chemical shift are correlated with the location of the shielded ligand proton within the base stack of the helix,[22,25] the NMR results described here also permit us to reexamine the geometric details of these proposed [Ru(phen)$_2$dppz]$^{2+}$ binding orientations. The original proposal[6] of a distribution of "side-on" and "head-on" intercalative orientations is based on several observations:[6,11] (i) The "light switch" effect is due to quenching of [Ru(phen)$_2$dppz]$^{2+}$ luminescence in aqueous solvent through proton association with the phenazine nitrogens; intercalation into the more hydrophobic base stack of DNA protects these ligand heteroatoms, thus preserving luminescence. (ii) [Ru(phen)$_2$dppz]$^{2+}$ complexes give rise to biexponential luminescence decays in emission consistent with some orientations in which one phenazine nitrogen was better protected than another, as would be expected for a "side-on" orientation. (iii) [Ru(NH$_3$)$_6$]$^{3+}$ quenches the shorter excited state decay component better than the longer lived component. (iv) The presence of D_2O has a greater effect on the shorter lifetime excited state.

Detailed three-dimensional structural models of the complexes bound to DNA are, of course, not possible to develop without extensive NOE constraints, yet given the rigidity of these complexes and the determination that they intercalate, we may explore and discriminate among possible stacking orientations based upon differential chemical shift information. The pattern of the 4′,7′ ligand proton resonances serves as our diagnostic tool. Using established correlations between upfield chemical shift changes due to ring current effects and the degree of penetration into the base stack,[22,25] we can examine models for intercalative stacking by these complexes which are consistent with the experimental data. These stacking models are provided in Figure 7. The relatively large size of the peak at 8.82 ($\Delta\delta$ −0.56 ppm from the free metal complex resonance) suggests an orientation in which both sides of the dppz ligand penetrate into the base stack to about the same extent. This pattern correlates nicely with the proposed "head-on" orientation. The remaining distribution of resonances is indicative of the inequivalence of the protons on either side of the dppz ligand in other binding orientations. In other words, one side of the dppz ligand is inserted into the base stack more deeply than the other side. Using the chemical shift changes −0.80 and −0.17 ppm as a guide for intercalation, a collection of very similar geometries, all of which are moderatively canted toward one strand, results. Since only purines can provide an upfield shift of −0.80 ppm, there is a preference for a geometry that maximizes stacking with an A or a G. This preference is of course also consistent with the A_5H8 intermolecular NOEs observed. Interestingly, molecular dynamics calculations based on NOESY data of Δ-α-[Rh[(*R*,*R*)-Me$_2$trien]phi]$^{3+}$−d(GAGTGCACTC)$_2$ also produce a preferred intercalative geometry between stacked purines on opposing strands.[17] Perhaps this geometry is generally favored for octahedral transition metal complexes.

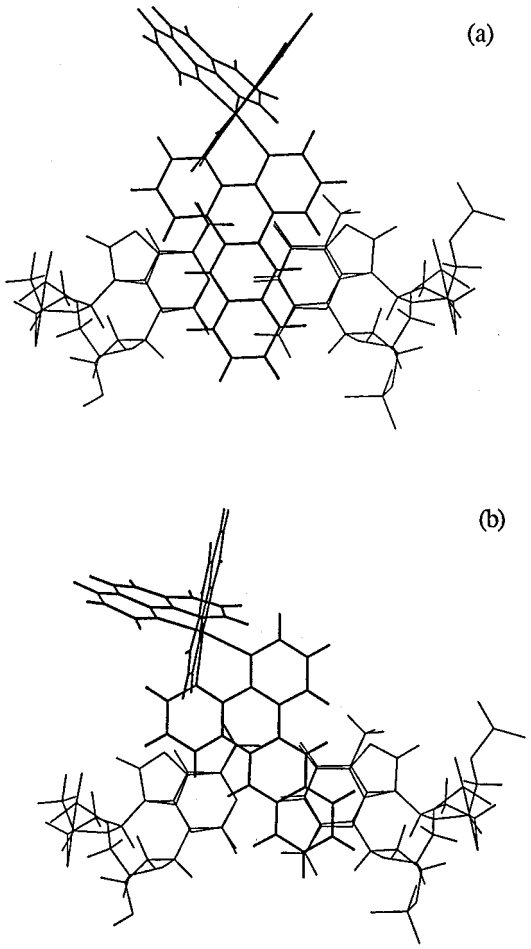

Figure 7. Models of intercalative binding based on chemical shift changes for 4,7′ dppz protons of Δ-[Ru(phen)$_2$dppz]$^{2+}$ when bound to d(GTCGAC)$_2$. The metal complex was docked into a d(GT)-d(AC)$_2$ duplex base step using correlations of ring current effects with upfield chemical shift change as a guide. Both models are consistent with a 4′,7′-A_5H8 intermolecular NOE and van der Waals requirements. Moderate chemical shift changes (≈−0.5 ppm) support a "head-on" mode (a) in which the dppz axis is perpendicular to both the base pair axis and the helical axis. Both phenazine nitrogens of the dppz ligand are comparably protected from aqueous solvent. The pairing of more substantially upfield shifted resonances (≈ −0.8 ppm) with slightly shifted resonances (≈−0.2 ppm) is consistent with a more asymmetric or canted intercalative geometry (b) in which the dppz axis of symmetry is more parallel to the base pair axis. This arrangement would afford more protection from aqueous solvent for one phenazine nitrogen than the other and is consistent with biexponential luminescence decay lifetimes.

Thus the NMR data clearly indicate geometries for intercalation in which the phenazine nitrogens of the dppz ligand are differentially exposed to solvent, a result consistent with luminescence data. The population of stacking geometries seen, as well as the sensitivity of these populations to enantiomeric substitution and modest dppz substitution (incorporation of fluorines), suggests that a low energy barrier exists between different intercalative stacking geometries. In light of the NMR data, the "head-on" and "side-on" binding geometries proposed

(43) Krotz, A. H.; Kuo, L. Y.; Shields, T. P.; Barton, J. K. *J. Am. Chem. Soc.* **1993**, *115*, 3877.

probably represent extremes in a spectrum of binding orientations sampled by the metal complex during intercalation.

Consolidation of Luminescence Results and NMR Structural Data. Luminescence studies provided initial evidence that [Ru(phen)$_2$dppz]$^{2+}$ intercalates into DNA.[2] Here we have confirmed this result and we have extended our understanding of the structural details of the enantioselective interactions of both Λ- and Δ-[Ru(phen)$_2$dppz]$^{2+}$ with the DNA oligonucleotide through the application of NMR spectroscopy. Several observations support intercalation by both isomers: (i) upfield changes in ^{1}H chemical shift for protons of the dppz ligand; (ii) characteristic downfield changes in ^{31}P chemical shifts for metal complex-bound duplex; (iii) increases in duplex melting temperature in the presence of both isomers. Upfield shifting and broadening of imino protons upon binding of the metal complex are also consistent with intercalation. Intermolecular NOEs furthermore position the Δ-isomer in the major groove.

NMR observations have furthermore been useful in detailing this intercalative stacking. Biexponential decays in luminescence for the ruthenium complexes bound to DNA provided initial support for multiple intercalative binding orientations. The movement of dppz ligand proton resonances upon binding DNA permitted us to clarify the details of this intercalative geometry, or indeed, population of geometries. Fluorine substitution on the dppz ligand leads to a deeper stacking interaction. The differences in 4′,7′ resonance patterns between bound enantiomers establish clearly that each bound intercalator samples a different set of stacked orientations. For the left-handed Λ- [Ru(phen)$_2$dppz]$^{2+}$, exchange with DNA appears faster compared to the Δ-isomer, a result which is consistent with its shorter DNA-bound excited state lifetimes. For the Δ-isomer, chemical shift information supports a collection of moderately canted binding orientations which represent the majority of interactions as well as a more symmetric uncanted orientation, which may correspond to the longest lived excited state luminescent component. This profile of orientations also provides an attractive explanation for the exchange broadened lines of this system. The consistency of intercalative models developed based upon NMR and luminescence data is also noteworthy given the different time scales for the two experiments. Importantly, these NMR data now provide a structural context for luminescence results and illustrate again the utility of NMR spectroscopy in describing metal complex−DNA interactions.

Acknowledgment. We are grateful to the NIH (Grant GM33309) for their financial support of this work. In addition C.M.D. thanks the NSF for a postdoctoral fellowship.

Supporting Information Available: Contour plots of the base-H1′ region of the NOESY spectrum of d(GTCGAC)$_2$ in the absence and presence of Δ-[Ru(phen-d_8)$_2$dppz]$^{2+}$ and a figure depicting the imino proton spectra of d(GTCGAC)$_2$ upon titration with [Ru(phen)$_2$dppz]$^{2+}$ (4 pages). See any current masthead page for ordering information.

IC960738A